Wideband Adaptive Beamforming Array With Improved Radiation Characteristics

Sathish Chandran, *Senior Member, IEEE*

***Abstract*—An efficient subband adaptive beamforming array (ABA) using a quadrature mirror filter (QMF) bank is presented. For wideband beamforming, taps have to be added to the full-band ABA for efficient suppression of the interference. However, the introduction of multiple taps results in the addition of uncorrelated noise to the ABA. This results in power loss in the direction perpendicular to the ABA. In order to compensate for the loss introduced by the addition of taps, the proposed concept is investigated. This configuration shows improved signal gain and deep suppression of the interference in the direction perpendicular to the ABA.**

***Index Terms*—Adaptive arrays, array signal processing, quadrature mirror filters (QMFs).**

I. Introduction

ADAPTIVE beamforming arrays (ABAs) are widely used to enhance the signal-to-noise ratio of any communication system. These arrays utilize the coherent addition of signals to obtain the required spatial selectivity. This makes the signals emanating from a particular look direction much stronger to detect. Works on ABA are becoming popular due to their inherent ability in suppressing interferences [1].

In a busy communication channel, the signals can be either narrowband or wideband. A wideband signal has a large bandwidth relative to its center frequency. If the signals are wideband, the phase shifting networks may not be sufficient to provide the desired output. This is because the complex envelope of the signal changes significantly across the extent of the array. The usual method for wideband array processing is based on introducing taps and then finding their appropriate weights for the beamforming process. However, the presence of more taps results in the addition of uncorrelated noise [2]. This can cause a reduction in the received power in the direction perpendicular to the beamforming array. The error introduced by the ABA would also affect the efficiency of the system. It has been shown that this error during the beamforming action can be reduced by dividing the bandwidth of the received signal into a number of subfrequency bands or subbands. The subband ABA techniques have already been introduced for narrowband signals [3] using quadrature mirror filter (QMF) banks. Recently, this technique has been applied to wideband signals [4], [5].

The reduced gain in the direction perpendicular to the ABA could be due to the cumbersome weight optimization procedure that has been performed for the entire bandwidth of the input signal. However, it is envisaged that the optimization for half of the entire bandwidth of the signal of interest would ease this burden.

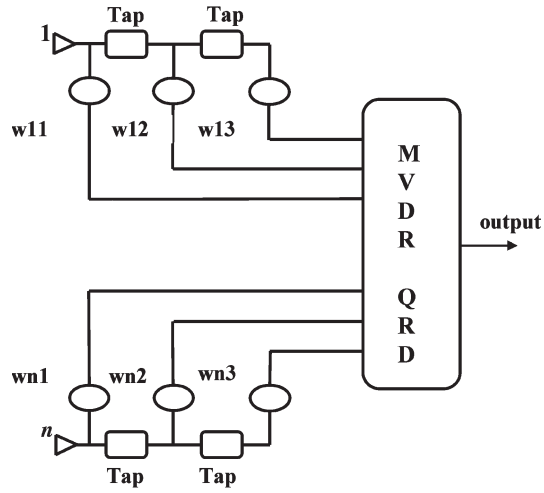

Fig. 1. Schematic diagram of the full-band ABA. w: weight of the associated taps.

In this letter, the ABA is subjected to investigation in view of improving the strength of the received signal in the direction perpendicular to the ABA. An eighth-order QMF bank is used in conjunction with the ABA to increase the power gain in the direction perpendicular to the ABA.

The subband array principles are discussed in Section II. In Section III, the problem formulation using the minimum-variance distortionless response (MVDR) method is outlined. Section IV deals with the simulation result of the subband ABA that is followed by the conclusions in Section V.

II. Subband ABA Principles

An ABA is a set of antennas organized in a certain pattern that utilize the spatial characteristics of the signal. It is often necessary to introduce a number of taps at the output of each sensor in a full-band adaptive array to increase the signal-to-noise ratio of the received wideband signals (Fig. 1). The properties of this type of ABA are utilized by varying the weight of each individual tap, which is computed iteratively from the received data.

When dealing with wideband signals, one has to opt for an ABA with more than one tap. This is required to determine the position of the null accurately. However, the more taps one uses, the higher the correlated noise would be [2]. This deteriorates the performance of the ABA. Applying beamforming over

Manuscript received January 15, 2003; revised July 20, 2004 and July 21, 2004; accepted October 27, 2004. The editor coordinating the review of this paper and approving it for publication is N. Mandayam.

The author is with the RF Consultants, 68100 Batu Caves, Selangor Darul Ehsan, Malaysia (e-mail: sathish@pc.jaring.my).

Digital Object Identifier 10.1109/TWC.2005.853885

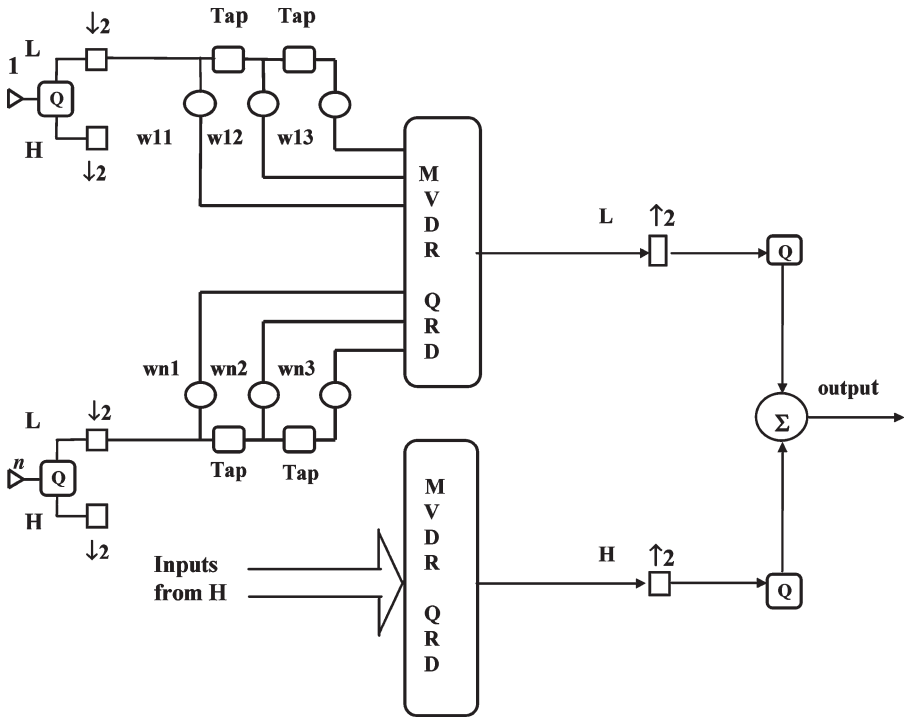

Fig. 2. Schematic diagram of the subband ABA. w: weight of the associated taps, Q: QMF, L: lower subband of the QMF output, H: higher subband of the QMF output, ↓2: decimation by 2, and ↑2: interpolation by 2.

adjacent subbands can alleviate this effect. The fast Fourier transform (FFT) algorithm is commonly used for this purpose. However, cross correlating these adjacent subbands can cause "aliasing." The application of QMF banks has been proposed [3] as an alternative solution to minimize the effect of aliasing, while QMF banks have been deployed in conjunction with the ABA (Fig. 2).

QMF banks are used in subband coding [6] to split the bandwidth of the incoming signal into two bands, each of which spans one half of the input bandwidth. These QMF banks can provide a sharp cutoff of the frequency spectrum [7]. The spectrum is divided into two subbands at the center frequency $f_s/4$, where f_s is the Nyquist frequency. The processes of the division of the input signal bandwidth into the lower and the higher subbands and the addition to the output signal bandwidth are schematically shown in Fig. 3. In the requirements illustrated in Fig. 2, the QMF banks are connected immediately after each antenna (analysis bank). This arrangement would help to retain the full information within the given bandwidth of the subband filter. Moreover, the higher subband signal response is the symmetrical to the lower subband signal response and vice versa. These optimized outputs are then interpolated by a factor of 2 and are recombined so that the errors introduced due to aliasing are to be decreased (synthesis bank). Since the data stream is decimated by a factor, which is greater than 1, it is envisaged that the computational complexity of the ABA can be reduced. The reason is that only every other sample is taken for computation.

In the application, an eighth-order QMF bank is employed in conjunction with the full-band ABA. It is believed that this will increase the strength of the received signal in the direction perpendicular to the antenna arrays while maintaining the effects of aliasing as low as possible. It is envisaged that such an ABA can be used effectively in any communication system that suffers from signal deterioration in the channel medium.

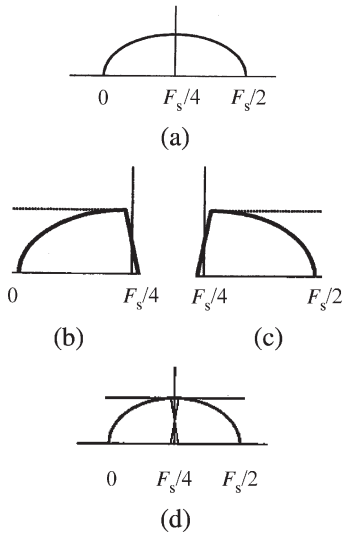

Fig. 3. Spectrum division and addition using QMF banks. (a) Spectrum of the input signal—before subbanding. (b) Spectrum of the lower subband signal—after subbanding. (c) Spectrum of the higher subband signal—after subbanding. (d) Spectrum of the output signal—after recombining.

MVDR [8] is used here for the computation of the ABA response. In this method, the variance or average power of the output is minimized under the constraint that a distortionless response is observed along the direction of a desired signal

and hence the name of the algorithm. The quadratic residue decomposition (QRD) has been used to implement the MVDR method efficiently and in an iterative manner [9], [10].

III. Subband ABA Techniques Using MVDR Method

A brief overview QRD-based MVDR algorithm is illustrated as follows. For an antenna array, the complex data value of the p antenna elements is given as

$$x(n) = (x_1(n), \ldots, x_p(n))^{\mathrm{T}} \tag{1}$$

where $x_j(n)$ denotes the jth antenna element at time n.

The algorithm begins by passing the output of each antenna through a two-channel filter bank. The resulting signals after decimation, by a factor 2, are of half the original rate.

Let $h_L(i)$ and $h_H(i)$ be the impulse responses of the lower and the higher subbands of the QMF banks. After downsampling, the bands are represented as

1) $y_L(n) = \sum_{i=1}^{I} h_L(i)x_j(n-i)$, for the lower subband, and
2) $y_H(n) = \sum_{i=1}^{I} h_H(i)x_j(n-i)$, for the higher subband; $y_{L_i}(n)$ and $y_{H_i}(n)$ are the lower and the higher subband outputs (snapshot) at time (n), where I is the order of the filter.

Also, define $Y_{L_i}(n)$ and $Y_{H_i}(n)$ as $1 \times n$ column vectors

$$Y_{L_i}(n) = (y_{L_i}(1), \ldots, y_{L_i}(n))^{\mathrm{T}} \tag{2a}$$

$$Y_{H_i}(n) = (y_{H_i}(1), \ldots, y_{H_i}(n))^{\mathrm{T}}. \tag{2b}$$

Data matrices Y_L and Y_H are expressed as $n \times p$ complex data matrices

$$Y_L(n) = \Lambda(n)\left(Y_{L_1}(n), \ldots, Y_{L_p}(n)\right) \tag{3a}$$

and

$$Y_H(n) = \Lambda(n)\left(Y_{H_1}(n), \ldots, Y_{H_p}(n)\right) \tag{3b}$$

where Λ is the $n \times n$ exponential weighing matrix and is given as

$$\Lambda(n) = \mathrm{diag}(\lambda^{n-1}, \ldots, \lambda^1 \quad 1) \tag{4}$$

where λ is the forgetting factor.

Since the algorithm is the same for both the higher and the lower subbands, here onwards only one band (higher band) is considered for the purpose of illustration.

Now the authors have to find the weight vector $w_L(n)$, for the lower band, which minimizes the cost function, which is expressed as a squared Euclidean norm

$$e(n) = \left\| \Lambda^{\frac{1}{2}}(n) Y_L(n) w_L(n) \right\|^2 \tag{5}$$

where $e(n)$ is the cost function, $Y_L(n)$ is the data matrix (lower band), and $w_L(n)$ is the tap weight vector (lower band), subject to a linear equality constraint $w_L^{\mathrm{H}}(n)s(\phi) = 1$, for all n, where $s(\phi)$ is the steering vector for a given electrical angle.

The response to this constrained optimization problem is described by the MVDR formula as [10]

$$\hat{w}_L(n) = \frac{\Phi_L^{-1}(n)s(\phi)}{s^{\mathrm{H}}(\phi)\Phi_L^{-1}(n)s(\phi)} \tag{6}$$

where $\hat{w}_L(n)$ is the estimate weight vector; H is the Hermitian transposition or the conjugate transposition; $s(\phi)$ is the steering vector, the electrical angle "ϕ" is determined by the look direction of interest; $\Phi_L(n)$ is the M-by-M correlation matrix of the exponentially weighted sensor outputs averaged over n snapshots and is related to the lower band data matrix Y_L as

$$\Phi_L(n) = Y_L^{\mathrm{H}}(n)\Lambda(n)Y_L(n) \tag{7}$$

where $\Phi_L^{-1}(n)$ is the recursive equation for the inverse of the correlation matrix and $\Phi_L(n)$ can also be written in terms of the matrix product $R_L^{\mathrm{H}}(n)R_L(n)$, where $R_L(n)$ is the upper triangular matrix that results from the application of the QRD to the exponentially weighted data matrix Y_L. Therefore, (6) can be rewritten as

$$\hat{w}_L = \frac{R_L^{-1}(n)R_L^{-\mathrm{H}}(n)s(\phi)}{s^{\mathrm{H}}(\phi)R_L^{-1}(n)R_L^{-\mathrm{H}}(n)s(\phi)} \tag{8}$$

where $R_L^{-\mathrm{H}}(n)$ is the Hermitian transpose of the inverse matrix $R_L^{-1}(n)$.

Let $a_L(n)$ be an auxiliary vector and defined as

$$a_L(n) = R_L^{-\mathrm{H}}(n)s(\phi). \tag{9}$$

Then (8) can be simplified as

$$\hat{w}_L = \frac{R_L^{-1}(n)a_L(n)}{a_L^{\mathrm{H}}(n)a_L(n)} \tag{10}$$

that is the solution for the weight.

The element pattern is assumed to be the same as the steering factor (vector). The subband mean-square error (MSE) is calculated as

$$e_{\mathrm{QMF}}(n) = d(n) - \hat{d}_{\mathrm{QMF}}(n) \tag{11}$$

where $d(n)$ is the desired response (signal); $\hat{d}_{\mathrm{QMF}}(n)$ is the estimate of the desired response (signal) and is given by

$$\hat{d}_{\mathrm{QMF}}(n) = h_L(i)^*\theta_L(n) + h_H(i)^*\theta_H(n) \tag{12}$$

in which $\theta_L(n) = w_L^{\mathrm{H}}Y_L(n)$ and $\theta_H(n) = w_H^{\mathrm{H}}Y_H(n)$, and $h_L(i)$ and $h_H(i)$ are the impulse responses of the lower and higher passbands of the QMF banks.

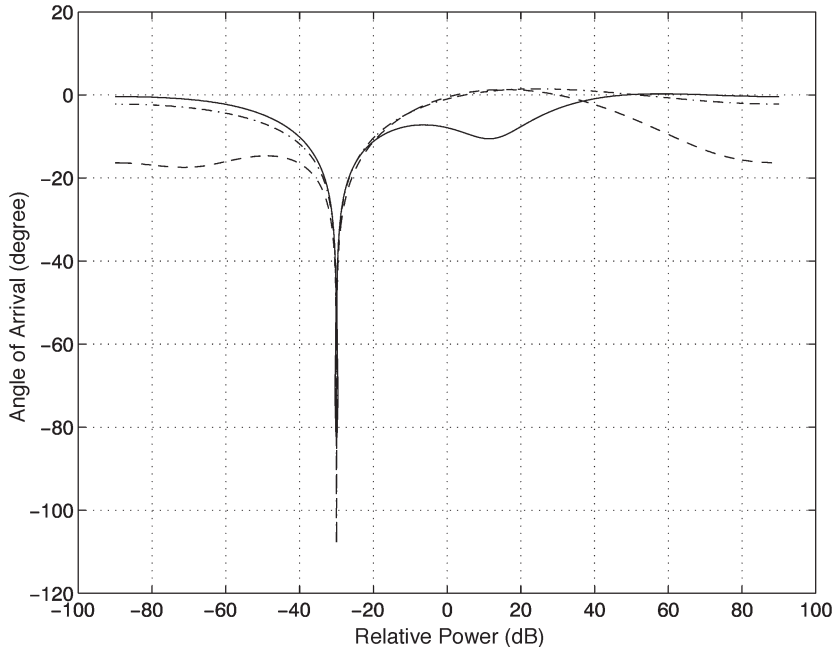

Fig. 4. Radiation patterns showing the desired and interference signals for the full-band and the subband ABAs. Thick line: full band. Dash: lower band of the QMF. Dashed dot: higher band of the QMF.

The components denoted by $R^{-1}(n)$ and $a(n)$ can be efficiently computed by a triangular systolic array based on the householder transformation. QRD [11] constitutes the fundamental component of the data-domain algorithm presented in [12], which has been applied to narrowband adaptive arrays for jammer cancellation. It operates recursively by using each snapshot of data to update an on-line estimate of the interferer.

According to the MVDR method, the weights multiplied by the steering vector are equal to one. Therefore, the MVDR method cannot be applied to cases in which the direction of the desired signal is not known. This method requires prior knowledge of the steering vector for the wanted signal and uses the covariance matrix R_n of the received signal for optimization.

IV. Simulation Results

The performance of the ABA system is evaluated for both the full-band and the subband cases. In the adaptive linear array structure, three consecutive antennas are placed at an interval of $\lambda/2$ each, where λ is the wavelength of the carrier frequency of the signal. The element antenna has an omnidirectional pattern. Four taps follow each antenna. The carrier frequency (f_c) is chosen arbitrarily and in this study is fixed at 8 MHz. The full bandwidth of $(2f_c)$ megahertz, i.e., 16 MHz, is assumed here for this investigation. The sampling rate is chosen to be four times the carrier frequency. The received signal is assumed to be a time-division multiple access (TDMA) signal with binary phase-shift keying (BPSK) modulation. It is also assumed that each antenna element contains zero mean thermal noise and they are uncorrelated with each other. The interference-to-noise ratio (INR) is assumed as 40 dB, which is assumed to be correlated. The interference comes from -30°, while the desired signal is from the direction perpendicular to the array (0°). An eighth-order finite impulse response (FIR)-QMF bank is used to split the signals into two subbands [13]. It has been found that the above QMF bank is the optimum since it gives less MSE during the beamforming process.

The ABA patterns of the full-band and the subband arrays are shown in Fig. 4. The desired full-band power is observed as approximately -8.0 dB at 0°. The corresponding values for the higher and lower subbands are noted as approximately -0.6 and -1.0 dB, respectively. Also, deep nulling is observed for the subband array than the full-band array. For the higher subband, the nulling level is obtained as deep as approximately -108 dB and for the lower subband is approximately -96 dB. For the full-band array, a nulling of approximately -84 dB has been noticed.

The (MSE) performance of the above ABAs has been looked into. The MSE values for all the ABA configurations are centered on approximately -85 dB (Fig. 5). It is worth noting that the reconstructed output after synthesis with the QMF banks shows almost the same MSE as that for the full-band array. The MSEs of the higher and the lower subbands are shown for ten iterations, since they are decimated by a factor of 2, after the QMF bank.

V. Conclusion

A full-band ABA for wideband applications was presented. A method to reduce the power loss in the direction perpendicular to the full-band ABA and the addition of multiple taps were investigated. To achieve this goal, an eighth-order FIR-QMF bank was used to split the incoming signals into two subbands.

The beamforming algorithm was then performed for these individual subbands. This approach resulted in the reduction of the power loss in the direction perpendicular to the ABA and improved the interference suppression of the full-band ABA. The power loss of the full-band ABA due to the introduction of

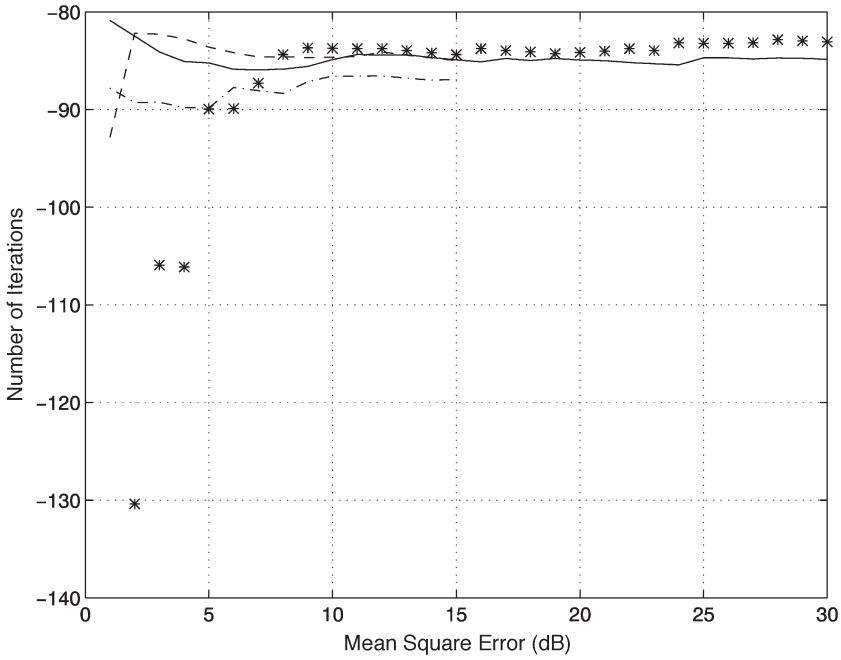

Fig. 5. Comparison of the MSEs between the full-band and the subband ABAs. Thick line: full band. Dash: lower band of the QMF. Dashed dot: higher band of the QMF. Star: reconstructed output.

taps was decreased for both the eighth-order FIR-QMF bank subband ABAs. It was also noted that the power loss in the direction perpendicular to the ABA had decreased as the order of the FIR-QMF bank was increased.

The reduced gain in the direction perpendicular to the ABA could be assumed due to the weight optimization that was performed for the entire bandwidth that was considered as cumbersome. This was assumed from the results that both antenna patterns of full-band beamforming and subband beamforming arrays had almost the same maximum directive gain as shown in Fig. 4.

Increased suppression for the interference was also noted for the both of the subband ABAs. It is also noted that as the order of the FIR-QMF bank was increased, the nulling depths of both bands of the subband ABA were decreased. As in the previous case, it was noted that the nulling levels were deeper than that of the full-band ABA.

Even after the band splitting, the MSE of both the subband ABAs remained the same as that for the full-band ABA (approximately -85 dB). The results discussed so far demonstrate that attenuated signals in the channel could be given more enhancement as well as efficient suppression of the interference prior to any signal processing within radio systems like sonar and radar systems. Thus, it justifies the candidacy of such an ABA system for a communication channel where the signal strength deteriorates rapidly.

REFERENCES

[1] *Adaptive Antenna Arrays: Trends and Applications*, S. Chandran, Ed. Berlin, Germany: Springer-Verlag, 2004.

[2] K. Farell, "Adaptive beamforming," in *Computational Methods of Signal Recovery and Recognition*, R. J. Mammone, Ed. New York: Wiley, 1992, ch. 10, series in Telecommunications.

[3] S. Chandran and M. K. Ibrahim, "Adaptive beamforming techniques using QMF," in *Proc. Int. Conf. Antennas and Propagation (ICAP, IEE)*, Eindhoven, The Netherlands, Apr. 4–7, 1995, pp. 257–260.

[4] ——, "Multirate sub-band adaptive beamforming using different kernel QMF banks," *Int. J. Electron.*, vol. 83, no. 1, pp. 119–132, 1997.

[5] S. Chandran, "A novel scheme for a sub-band adaptive beamforming array implementation using quadrature mirror filter banks," *Electron. Lett.*, vol. 39, no. 12, pp. 891–892, 2003.

[6] V. K. Jain and R. E. Crochiere, "Quadrature mirror filter design in the time domain," *IEEE Trans. Acoust. Speech Signal Process.*, vol. ASSP-32, no. 2, pp. 353–361, Apr. 1984.

[7] P. P. Vaidyanathan, *Multirate Systems and Filter Banks*. Englewood Cliffs, NJ: Prentice-Hall, 1992.

[8] J. G. McWhirter and T. J. Shepherd, "Systolic array processor for MVDR beamforming," *Proc. Inst. Elect. Eng.*, vol. 136, no. 2, pp. 75–80, 1989.

[9] S. Haykin, *Adaptive Filter Theory*. Englewood Cliffs, NJ: Prentice-Hall, 1991.

[10] D. Kahaner, C. Moler, and S. Nash, *Numerical Methods and Software*. Englewood Cliffs, NJ: Prentice-Hall, 1989.

[11] G. H. Golub and C. F. Van Loan, *Matrix Computations*. Baltimore, MD: John Hopkins Univ. Press, 1983.

[12] C. R. Ward, P. J. Hargrave, and J. G. McWhirter, "A novel algorithm and architecture for adaptive digital beamforming," *IEEE Trans., Antennas Propag.*, vol. AP-34, no. 3, pp. 338–346, Mar. 1986.

[13] J. D. Johnston, "A filter family designed for use in quadrature mirror filter banks," in *Proc. Int. Conf. Acoustics, Speech and Signal Processing (ICASSP)*, Albuquerque, NM, Apr. 1990, pp. 291–294.